

ReViP: Reducing False Completion in Vision-Language-Action Models with Vision–Proprioception Rebalance

Zhuohao Li^{1,2} Yinghao Li^{1,2} Jian-Jian Jiang¹
 Lang Zhou^{1,2} Tianyu Zhang^{3,2} Wei-Shi Zheng^{1,4,5,6}✉

¹Sun Yat-sen University ²Shenzhen Loop Area Institute

³Beijing Institute of Technology ⁴Peng Cheng Laboratory, China

⁵Key Laboratory of Machine Intelligence and Advanced Computing, Ministry of Education, China

⁶Guangdong Province Key Laboratory of Information Security Technology, China

lizhh268@mail2.sysu.edu.cn; wszheng@ieee.org

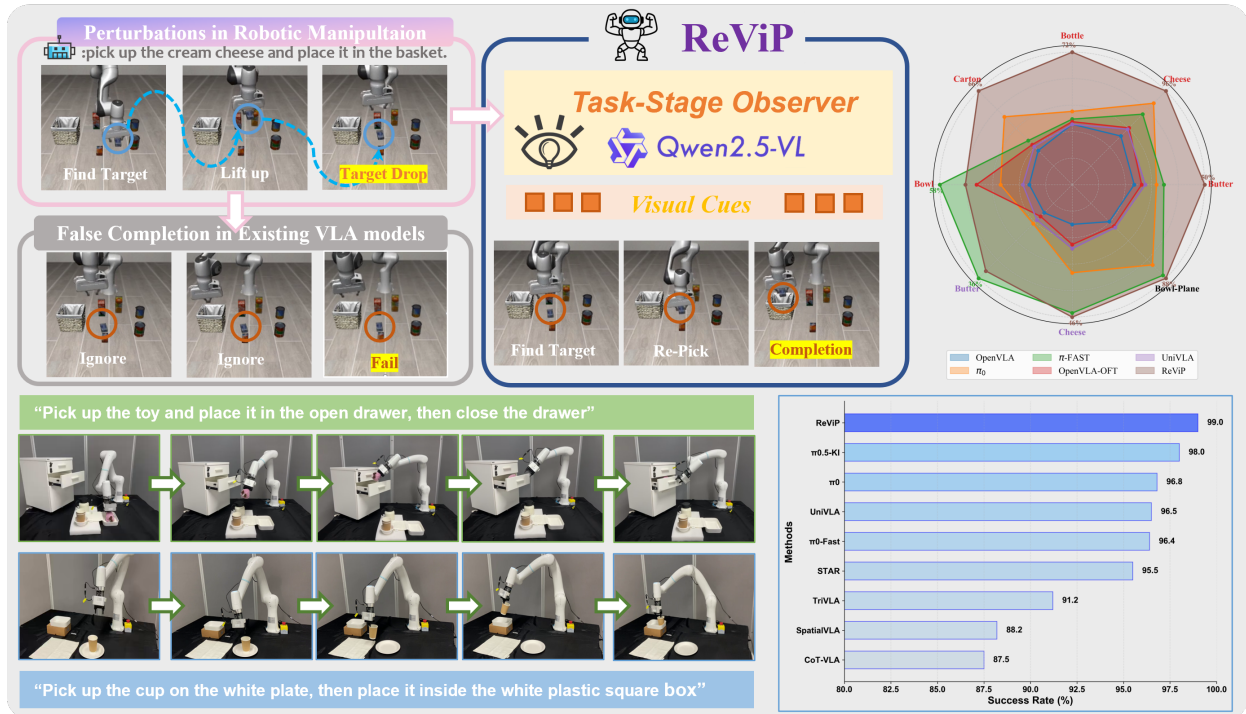


Figure 1. **Rebalancing Vision & Proprioception.** Under unexpected perturbations such as object drops, existing VLA models may exhibit false completion by prioritizing internal state progression over visual feedback. By injecting task-stage cues, ReViP rebalances semantic perception and proprioceptive dynamics, enabling the policy to identify the object, re-pick it, and complete the task, leading to consistent performance improvements across simulation benchmarks and real-world experiments.

Abstract

Vision-Language-Action (VLA) models have advanced

✉ corresponding authors.

robotic manipulation by combining vision, language, and proprioception to predict actions. However, previous methods fuse proprioceptive signals directly with VLM-encoded vision-language features, resulting in state-dominant bias

and false completions despite visible execution failures. We attribute this to modality imbalance, where policies over-rely on internal state while underusing visual evidence. To address this, we present **ReViP**, a novel VLA framework with **Vision-Proprioception Rebalance** to enhance visual grounding and robustness under perturbations. The key insight is to introduce auxiliary task-aware environment priors to adaptively modulate the coupling between semantic perception and proprioceptive dynamics. Specifically, we use an external VLM as a task-stage observer to extract real-time task-centric visual cues from visual observations, which drive a **Vision-Proprioception Feature-wise Linear Modulation** to enhance environmental awareness and reduce state-driven errors. Moreover, to evaluate false completion, we propose the first **False-Completion Benchmark Suite** built on LIBERO with controlled settings such as **Object-Drop**. Extensive experiments show that ReViP effectively reduces false-completion rates and improves success rates over strong VLA baselines on our suite, with gains extending to LIBERO, RoboTwin 2.0, and real-world evaluations.

1. Introduction

The development of Vision-Language-Action (VLA) models [12, 14, 17, 27, 28, 34] have demonstrated impressive progress in robotic manipulation. These models are constructed by integrating pre-trained visual-language encoders with proprioceptive feedback to predict actions, enabling generalization across a wide range of robotic tasks [2, 32].

Despite encouraging progress, previous methods typically encode visual-language inputs via Visual-Language Models (VLMs) and directly fuse proprioceptive signals [5, 18], leading to state-dominant bias and false completions even in the presence of clear visual failure cues. We attribute this behavior to modality imbalance, where policies over-rely on internal state while underusing visual evidence. For instance, when a target object drops during the execution, the policy continues the planned placement action towards the goal region, despite the target remaining visible and requiring retrieval. As shown in Figure 1, the policy may prematurely halt or incorrectly declare success when the goal is unmet, causing the robot to terminate the operation without further action. We term this phenomenon **False-Completion**. This behavior suggests that visual feedback is underutilized, with decision-making processes relying on proprioceptive cues, which conflicts with human common-sense task completion reasoning. However, few studies explicitly explore the imbalance between visual evidence and proprioceptive progression in VLA models, and the phenomenon of false completion remains significantly underexplored.

To address this, we present ReViP, a VLA framework

that enhances visual grounding and robustness under perturbations by rebalancing vision perception with proprioceptive dynamics. To be specific, ReViP constructs a **Task-Stage Observer** based on an external VLM to process the current observation and instruction, extracting real-time task-centric visual cues that reflect task progress and environmental state. These cues serve as auxiliary task-aware environment priors. Building on this, the **Task-Stage Enhancer** is introduced to inject these priors into the policy via a **Vision-Proprioception Feature-wise Linear Modulation**, adaptively rebalancing semantic perception and proprioceptive dynamics at the feature level. This design not only promotes feedback awareness but also mitigates state-driven errors under perturbations, such as object drops, distractor-induced mismatches, and environment re-layout. Additionally, we introduce the **False-Completion Benchmark Suite**, a simulation benchmark on the LIBERO platform [22], designed to systematically evaluate the performance of VLA models under false-completion perturbations. The suite includes three controlled perturbation settings: object drop, distractor swap, and relayout, each targeting a different aspect of model robustness. The object drop task evaluates the model’s response to dynamic disruptions, while the distractor swap task tests its ability to distinguish between targets and distractors. The relayout task challenges the model’s adaptability to variations in the environment layout.

We conduct extensive experiments across several simulation benchmarks, including false-completion evaluation, the standard LIBERO, and the dual-arm RoboTwin 2.0 benchmark [8], covering a diverse set of robotic manipulation tasks. In addition, real-world experiments are performed to further validate our hypothesis. The results demonstrate that ReViP significantly reduces false completions under unseen disturbances and achieves state-of-the-art (SOTA) task success rates, consistently outperforming existing methods on these challenging tasks. Our contributions can be summarized as follows:

- We identify a failure mode rooted in modality imbalance in VLA models, which leads to a state-dominant bias and *false completion*.
- We propose *ReViP* inspired by the idea of vision-proprioception rebalance, which includes a task-stage observer to provide additional task-stage semantic feedback and a task stage enhancer that adaptively strengthens the visual stream at the feature level.
- We introduce *False-Completion Benchmark Suite* tailored for evaluating false completion under controlled settings, including *drop*, *swap*, and *relayout*.
- We demonstrate consistent reductions in false completion rate and improvements in task success rate over other VLA models, with benefits that extend to LIBERO, RoboTwin 2.0 benchmark, and real-world experiments.

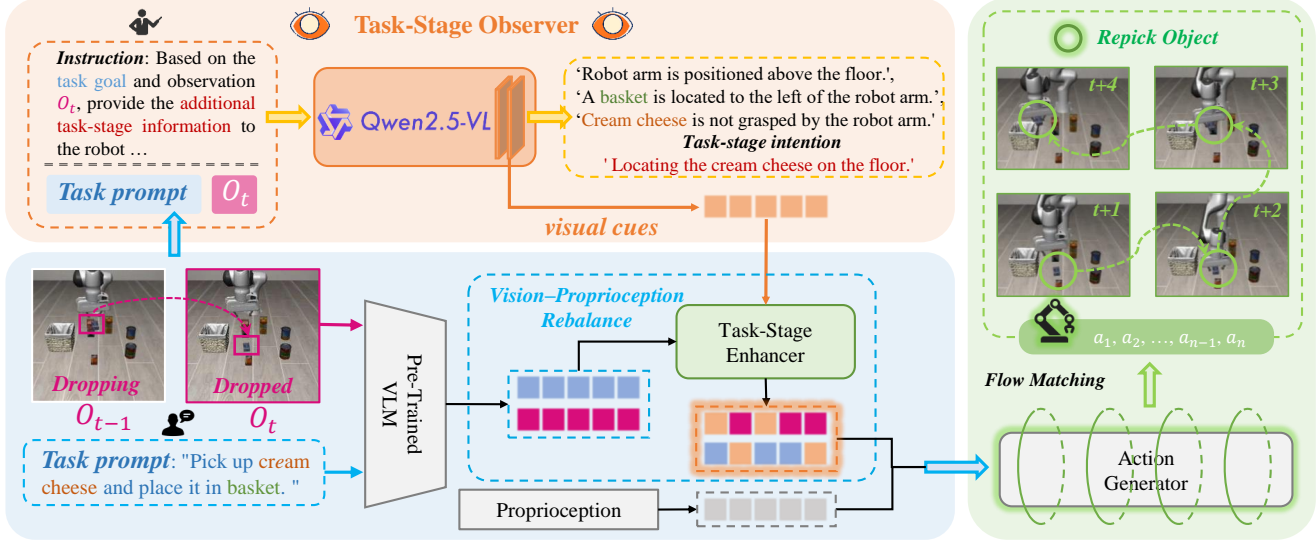


Figure 2. Overview of the proposed ReViP framework. It consists of two stages: (above) Task-Stage Observer for cues extraction and (below) Task-Stage Enhancer for rebalancing. Through a frozen vision–language model (Qwen 2.5), task–centric visual cues are extracted from the observation O_t and task instructions. These cues are then injected into the VLA backbone by the Task-Stage Enhancer to adaptively rebalance the visual and proprioceptive streams.

2. Related Work

Vision-Language-Action Models. VLA models [5, 12, 27, 34] connect perception to control by mapping pre-trained vision-language representations to executable actions. Early approaches in the RT line (RT-1 [6], RT-2 [34], RT-H [4]) introduced action tokenization and trained transformer policies from scratch on large-scale demonstration corpora such as Open X-Embodiment [26] and DROID [2]. Recently, the π series (FAST [27], π_0 [5], and $\pi_{0.5}$ [14]) proposed heterogeneous co-training across robots and used flow matching-based decoders [21] for continuous action generation. The π series (FAST [27], π_0 [5], $\pi_{0.5}$ [14]) adopted heterogeneous co-training across robots and flow-matching decoders [21] for continuous action generation. Beyond these, a range of VLA variants [12, 19, 20, 24, 28, 32] explore performing better robot manipulation, including structured reasoning, spatial grounding, and efficient architectures. For example, CoT-VLA [32] integrates chain-of-thought style reasoning with a lightweight policy to improve efficiency. In contrast to these methods, we investigate a different challenge: *modality imbalance* in VLA models, where proprioceptive progress tends to dominate visual feedback. This state-dominant bias leads to a failure mode (false completion) that our method explicitly targets.

VLA Models with External VLMs. Directly fine-tuning the VLM inside a VLA on robot data often degrades its pre-trained multimodal understanding because of distribution shift and forgetting [5, 14, 33], which motivates keeping a strong external VLM for task understanding [11]. Recent

methods fall into two patterns. The first uses the VLM to decompose long-horizon instructions into subgoals, leaving the VLM only as a planner without exposing its internal semantic features to the VLA backbone [1, 13]. The second uses the VLM as a goal or step judge to decide success and trigger handcrafted retries or resets, which requires task-specific flows and incurs expensive restarts [9, 10]. Differing from them, our proposed ReViP injects internal VLM representations into the VLA via task-stage feedback mechanisms to rebalance vision and proprioception.

3. ReViP

In this section, we describe how our ReViP addresses the false completion problems. First, we give a definition of the false completion phenomena and revisit our motivation (Section 3.1). Then, we introduce the Task Stage Observer, which distills observations and instructions into task-centric visual cues (Section 3.2) and the Task Stage Enhancer, which injects these cues into the VLA and rebalances visual–proprioceptive signals (Section 3.3). Finally, we summarize the overall structure of ReViP (Section 3.4).

3.1. Problem Setup & Motivation

False Completion. Here, we formalize the setting of false completion. The observation I_t at time step t consists of synchronized images from a set of cameras \mathcal{C} that include egocentric and exocentric views:

$$I_t = \{I_t^{(c)} \in \mathbb{R}^{H_c \times W_c \times 3} \mid c \in \mathcal{C}\}. \quad (1)$$

The policy π_θ then predicts a block of n future actions (action chunk) as follows:

$$A_t = \pi_\theta [a_t, a_{t+1}, \dots, a_{t+n-1} \mid (I_t, S_t, l)]. \quad (2)$$

Here, proprioception and instruction are denoted by S_t and l respectively. Then, a termination flag $d_t \in \{0, 1\}$ is defined, where $d_t = 1$ is a completion declaration by the policy. Let $G(I_t) \in \{0, 1\}$ be a visual goal predicate decided from the multi-view images. Following that, a task instance is considered truly completed only when both the policy declares completion and the visual predicate confirms goal satisfaction. However, when the policy issues a completion declaration while a visual predicate indicates the goal is unmet, we obtain a **false completion**, that is:

$$\begin{aligned} \text{True Completion} &= [d_t = 1 \wedge G(I_t) = 1], \\ \text{False Completion} &= [d_t = 1 \wedge G(I_t) = 0]. \end{aligned} \quad (3)$$

Motivation. In this work, we attribute this failure mode to a modality imbalance in current VLA models, which favors proprioceptive progress over multi-view visual evidence. The modality imbalance in VLA models induces a state-dominant bias. Therefore, when perturbations occur, like objects dropping, the robot may ignore the change in observation I_t and keep the ongoing execution, which results in false completion. The key insight of ReViP, which achieves the shift from false to true completion, is to extract explicit task-centric visual cues from observations and rebalance the influence of vision and proprioception at decision time.

3.2. Task-Stage Observer

To address modality imbalance where visual information is underused, we propose the Task-Stage Observer (TSO) to convert raw observations and instructions into task-centric visual cues while explicitly filtering task-irrelevant content. In our implementation, we employ a Qwen 2.5-VL [3] as the representative vision–language backbone for the TSO.

At time step t , TSO takes the observation I_t and instruction l as inputs, and performs a goal-grounded analysis that first identifies the robot’s currently visible physical state and the spatial location and status of the task-relevant objects, then infers the immediate stage intention aligned with the given goal. The resulting cues provide explicit visual evidence for decision-making and generate a concise hypothesis for the subsequent task stage. As illustrated in the representative *object drop* scenario (Figure 2), when the target *cream cheese* accidentally falls while the robot is moving toward the basket from I_{t-1} to I_t , TSO analyzes (I_t, l) to produce critical task-stage evidence such as “*Cream cheese is not grasped by the robot arm*”. These cues establish that the target is no longer held by the gripper and localize it within the scene. By localizing the dropped object and generating a new stage intention, e.g., “*Locating the cream*

cheese on the floor”, the TSO guides the policy to initiate a re-pick action instead of continuing toward the basket, as is commonly observed in baseline VLA models.

To inject these discrete language cues into the VLA backbone, we adopt an LLM-based embedding extraction strategy [16, 25, 29, 30] that converts the last layer hidden states into a compact continuous feature:

$$z_t = \text{Proj} \left(\text{Pool}(\text{TSO}_L(I_t, l)) \right) \in \mathbb{R}^d, \quad (4)$$

where L denotes the last layer of the external VLM, $\text{Pool}(\cdot)$ aggregates the selected token representations into a single vector, and $\text{Proj}(\cdot)$ is a linear projection that maps this vector to the VLA semantic space of dimension d .

3.3. Task-Stage Enhancer

Building upon the Task-Stage Observer, we introduce a Task-Stage Enhancer (TSE) to strengthen task-relevant visual features and to rebalance the relative influence of vision and proprioception during action generation.

The TSE first translates the extracted task-stage cues z_t into adaptively controlled signals via task-stage feature-wise linear modulation (TS-FiLM). This mechanism ensures that decision-making is driven by current task-centric visual cues rather than an inertial reliance on internal state, which directly targets the false-to-true completion shift. Specifically, given z_t , the TSE produces feature-wise modulation parameters through a compact bottleneck mapping $h(\cdot)$, which can be expressed as:

$$[\gamma_t, \beta_t] = h(z_t), \quad (5)$$

where $\gamma_t, \beta_t \in \mathbb{R}^D$, and D is the token hidden size of the VLM backbone in VLA models. In the ReViP framework, let $P_t \in \mathbb{R}^{B \times S \times D}$ represent the concatenated vision and language prefix tokens, accompanied by a binary validity mask $M_t \in \{0, 1\}^{B \times S}$. We then apply token-wise TS-FiLM to the vision-language prefix before action generation. Therefore, TSE generates modulated prefix tokens \tilde{P}_t before action prediction:

$$\tilde{P}_t = \left(P_t + \alpha (\gamma_t \odot P_t + \beta_t) \right) \odot M_t, \quad (6)$$

where $\alpha \in \mathbb{R}_+$ is a learnable modulation factor and \odot denotes Hadamard product over tokens. This operation performs feature-level injection of task-centric visual cues, effectively amplifying channels aligned with visual evidence while attenuating distractors that contribute to state-dominant bias.

3.4. Overall

Action Prediction. The action head is trained to predict a conditional velocity field $v_\theta(\cdot, \cdot \mid \tilde{F}_t)$ via flow matching on the modulated prefix \tilde{F}_t . For a ground-truth action chunk A_t

Table 1. **Experimental Results of False-Completion Benchmark.** Success rates (SR) and average ranks (RK) across eight tasks grouped into three perturbation sources: Object Drop, Distractor Swap, and Relayout. \clubsuit indicates non-tabletop cabinet scenes (i.e., cabinet scenes). The best result is shown in **bold**. ReViP achieves the highest average SR and the best RK across the benchmark.

Methods	Object-Drop					Distractor-Swap		Relayout		Average	
	Butter	Cheese	Bottle	Carton	Bowl \clubsuit	Butter	Cheese	Bowl-Plane	SR \uparrow RK \downarrow		
									SR \uparrow	RK \downarrow	
OpenVLA [17]	12%	30%	16%	6%	2%	0%	0%	12%	10%	6	
π_0 [5]	24%	78%	26%	40%	20%	6%	24%	70%	36%	2	
π_0 -Fast [27]	28%	62%	20%	16%	58%	36%	44%	84%	44%	3	
OpenVLA-OFT [18]	16%	42%	18%	12%	35%	2%	10%	18%	19%	4	
UniVLA [7]	18%	40%	16%	10%	6%	4%	12%	20%	18%	5	
ReViP	50%	96%	72%	66%	42%	32%	46%	88%	62%	1	

and random noise ε , we sample $\tau \sim \mathcal{U}(0, 1)$ and construct a noisy interpolation along the straight-line path:

$$v_\tau = (1 - \tau)A_t + \tau\varepsilon, \quad (7)$$

The target velocity (i.e., the time derivative of this path) is:

$$u_\tau = \frac{dv_\tau}{d\tau} = \varepsilon - A_t, \quad (8)$$

Above all, the training objective regresses the predicted velocity onto this target:

$$\begin{aligned} \tilde{F}_t &= \text{Fusion}(\tilde{P}_t, S_t), \\ \mathcal{L}_{\text{FM}} &= \|v_\theta(v_\tau, \tau \mid \tilde{F}_t) - u_\tau\|_2^2. \end{aligned} \quad (9)$$

When a perturbation such as an object drop occurs, z_t steers $[\gamma_t, \beta_t]$ to highlight the dropped object evidence and suppress irrelevant content, which guides the action generator toward approach and regrasp rather than proceeding to the goal region, thereby reducing false completion.

Overall Framework. Bringing all together, our ReViP framework is developed. As shown in Figure 2, it processes the input observation and language instruction through the Task Stage Observer, which first distills them into task-centric cues identifying relevant objects and stage intent. Then, the Task Stage Enhancer injects these visual cues into the VLA backbone via TS-FiLM, enhancing VLM-derived features while adaptively rebalancing visual and proprioceptive signals. Finally, the resulting modulated representation conditions a flow matching-based action generator to predict an action chunk in parallel, yielding the output of precise robotic actions.

4. Experiments

In this section, we first introduce our False-Completion Benchmark Suite (Section 4.1). We then evaluate ReViP

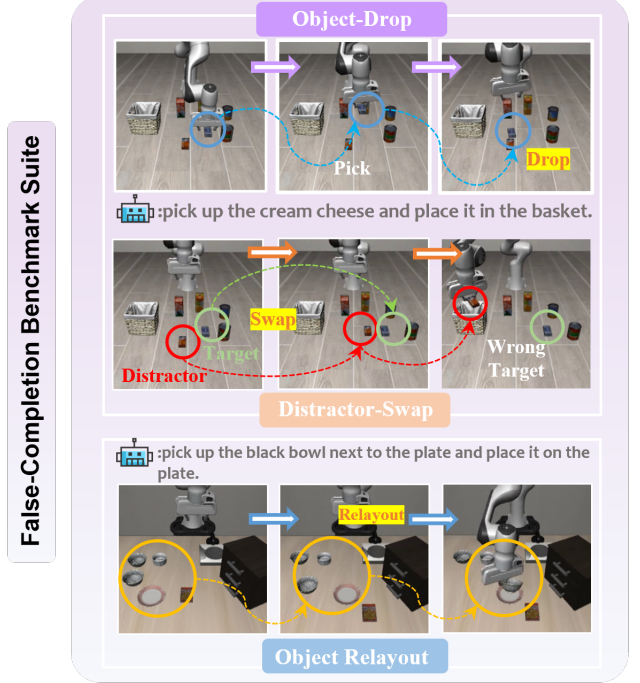


Figure 3. Illustrative examples of our False Completion Benchmark. The benchmark consists of three complementary perturbation sources. Object drops assess whether the policy can detect failures that occur during execution. Distractor swaps examine instance-level grounding under visually similar objects. Relayout conditions test spatial reasoning when the target and its goal appear in new configurations.

across simulation benchmarks (Section 4.2-4.4), and real-world settings (Section 4.5) to measure robustness to false completion and general manipulation performance.

4.1. False-Completion Benchmark Suite

False completion arises when external disturbances or unintended robot actions invalidate the ongoing plan while the

Table 2. **Experimental Results of Simulation Experiments on the LIBERO benchmark.** Success rates (SR) and average ranks (RK) across four task suites: LIBERO Spatial, Object, Goal, and 10. The best result is shown in **bold**, and ReViP reaches the highest average SR and the best RK across all suites.

Methods	Spatial		Object		Goal		10		Average	
	SR \uparrow	RK \downarrow								
SpatialVLA [28]	88.2	8	89.9	7	78.6	8	55.5	9	78.1	7
π_0 [5]	96.8	3	98.8	1	95.8	2	85.2	5	94.2	4
π_0 -Fast [27]	96.4	5	96.8	4	88.6	6	60.2	8	85.5	5
CoT-VLA [32]	87.5	9	91.6	6	87.6	7	69.0	7	83.9	6
STAR [19]	95.5	6	98.3	2	95.0	4	88.5	3	94.3	3
$\pi_{0.5}$ -KI [14]	98.0	2	97.8	3	95.6	3	85.8	4	94.3	3
TriVLA [24]	91.2	7	93.8	5	89.8	5	73.2	6	87.0	5
UniVLA [7]	96.5	4	96.8	4	95.6	3	92.0	2	95.2	2
ReViP	99.0	1	98.8	1	96.6	1	92.2	1	96.7	1

Table 3. **Experimental Results of the Dual-Arm RoboTwin 2.0 benchmark** (Hard mode evaluation). Success rates are reported. The best result is shown in **bold**.

Task	DP3	RDT	π_0 [5]	ReViP
Place Object Stand	0%	5%	11%	20%
Place Bread Basket	1%	2%	4%	13%
Pick Dual Bottles	1%	13%	12%	20%
Put Bottles Dustbin	21%	4%	13%	26%
Average	4%	4%	7%	14%

robot still declares success. To study state-dominant bias and visually apparent false completions in a controlled manner, we build a False-Completion Benchmark Suite based on LIBERO that injects targeted perturbations and probes complementary aspects of the phenomenon.

In this paper, we consider three perturbation sources that commonly induce false completion: Object Drop, Distractor Swap, and Object Relayout. Together, they form a suite of eight tasks that constitute the proposed False Completion Benchmark. As shown in Figure 3, each perturbation family targets a distinct failure mode of state-driven policies: drops test the ability to detect mid-execution failures, swaps probe instance-level grounding under similar objects, and relayout conditions evaluate spatial reasoning when both the target and its goal appear in new configurations.

Specifically, the instruction remains fixed while only the environment is perturbed at the start of the episode or during execution. This disturbance design prevents success via replaying demonstration-like proprioceptive trajectories and instead compels policies to rely on current visual evidence for progress checking and replanning. Therefore, our suite provides a controlled setting for evaluating the robustness of models against false completion. Below, we will introduce three types of perturbation sources.

Object Drop. This setting, which includes Small Object Drop, Large Object Drop, and Bowl Drop in Cabinet, tests recovery from unexpected displacement and exposes false completion most directly. Three variants are instantiated that differ in object scale and contact context.

Distractor Swap. This setting evaluates whether the policy detects that two visually similar objects have swapped positions, rather than replaying a proprioceptive-driven trajectory. The initial poses of the target and a visually similar distractor are swapped, while the instruction remains fixed.

Object Relayout. This setting disrupts demonstration-specific spatial priors while preserving the linguistic target. The target object and its goal region are jointly relocated to new feasible positions. The policy is therefore required to update its plan based on current visual evidence, instead of relying on stale internal state.

In conclusion, the benchmark suite emphasizes visual grounding, continuous progress monitoring, and effective replanning under distribution shifts that often result in false completions, offering a focused and diagnostic evaluation framework for VLA models. Further details can be found in the supplemental materials.

4.2. Simulation Benchmark Experiment.

We evaluate ReViP in two key aspects: First, the robustness of ReViP is assessed using our False Completion Benchmark Suite, which applies controlled perturbations to induce state-dominant bias and false completions. Next, we further evaluate ReViP on the widely used LIBERO [22] and the RoboTwin 2.0 benchmark [8] for generalization verification, covering diverse scenes and task categories.

Implementation Details. For all experiments, we use π_0 , a representative VLA framework, as the backbone policy for ReViP. The Task-Stage Observer is instantiated with Qwen2.5-VL 72B to extract instruction-conditioned task-stage cues. Training is conducted on 8 \times H100 GPUs, with

a total batch size of 32 over 60k training steps.

Baselines. We compare ReViP with representative VLAs, including OpenVLA [17], OpenVLA-OFT [18], SpatialVLA [28], π_0 [5], π_0 -Fast [27], CoT-VLA [32], TriVLA [24] and UniVLA [7] in single-arm settings. For a more challenging bimanual-arm setting, we further evaluate DP3 [31], RDT [23] and π_0 on the RoboTwin 2.0 benchmark [8].

4.3. Evaluation on False-Completion Benchmark

Quantitative Results. Table 1 presents a comparative evaluation of existing VLA methods on the False Completion benchmark. ReViP achieves the highest average success rate of 62% and the best average rank across all eight tasks, outperforming the strongest baseline, π_0 -Fast, by 18% and the baseline model, π_0 , by 26%. This aggregate improvement demonstrates that rebalancing visual and proprioceptive inputs with task-centric cues consistently enhances performance across diverse perturbations.

In Object Drop tasks, where policies must detect failures rather than follow an inertial plan, ReViP achieves an average success rate of 65.2% across five drop tasks, outperforming other VLAs. This demonstrates that the task-stage observer enhances visual failure detection and replanning, preventing the blind continuation of proprioception-driven progress. In Distractor Swap tasks, where object recognition and manipulation are confused, ReViP outperforms both π_0 and π_0 -Fast by 15% and 40% respectively. These results suggest that task-stage cues help disambiguate visually similar instances, highlighting ReViP’s superior scene understanding in distraction-heavy tasks. In Relayout tasks, which emphasize global layout reasoning when both the target and its goal region are shifted, ReViP achieves the highest success rate of 88%. This clearly surpasses both π_0 and UniVLA, showing ReViP’s advantage in tasks that require precise spatial reasoning and fine-grained object control.

All these gains indicate that the injected task stage cues help the policy rely less on demonstration-specific spatial priors and more on the current visual configuration, in line with our vision and proprioception rebalance objective.

Qualitative Results. Figure 4 presents a representative comparison between ReViP and π_0 under the Object Drop perturbation. When the bottle slips from the gripper, π_0 continues its proprioception-driven trajectory, ignoring the visible failure and ultimately declaring a false completion. In contrast, ReViP immediately responds to the drop event, triggers a re-pick attempt, and guides the policy to replan, recover the object, and successfully complete the task. This qualitative behavior highlights the mechanism behind ReViP’s performance gains on the False Completion Benchmark: decisions are based on the current visual observation rather than on internal proprioceptive progress.

Along with the numerical improvements in Table 1, these qualitative results demonstrate that ReViP consis-

tently transforms failure cases, which typically trap the baseline VLA model, into successful recoveries through vision-proprioception rebalancing during execution.

4.4. Evaluation on General Simulation Benchmark

Performance on LIBERO. As shown in Table 2, we evaluate ReViP on the LIBERO benchmark, including LIBERO-Spatial, LIBERO-Object, LIBERO-Goal, and LIBERO-10 (also called LIBERO-Long), each with 10 tasks and 50 demonstrations. ReViP consistently outperforms all other models, achieving the highest average task success rate of 96.7%, surpassing both UniVLA and the backbone model π_0 . Specifically, on LIBERO-Spatial, ReViP reaches 99.0% success, effectively saturating the suite and slightly improving on the best existing methods. On the more challenging LIBERO-10 suite, which involves long-horizon manipulation across mixed task families, ReViP improves π_0 ’s success rate from 85.2% to 92.2%, a 7% gain, demonstrating better stability over extended executions.

These results indicate that the proposed vision and proprioception rebalance with task stage cues not only mitigates false completion, but also improves performance on standard manipulation tasks without explicit perturbations.

Performance on RoboTwin 2.0 (Dual Arm). To further assess the performance of ReViP extended to two-arm settings, we evaluate on the RoboTwin 2.0 benchmark, which features contact-rich dual-arm manipulation. We consider four representative tasks in a single task training setup, each trained with 50 demonstrations collected in clean environments. Evaluation is performed under *hard mode conditions* with 100 trials per task, incorporating domain randomization, lighting variations, object clutter, and table height shifts. Detailed results provided in Table 3, ReViP achieves the highest average success rate and outperforms compared methods, such as RDT and the baseline π_0 . This indicates that the task-stage feedback mechanism in ReViP scales effectively to dual-arm tasks and remains robust under severe environmental perturbations, supporting our claim that explicit environmental feedback enhances policy robustness.

4.5. Real-World Experiment

Robot platform. Our real-world experiments are conducted using a 6-dof ROKAE robotic arm equipped with a JODELL gripper. During the data collection phase, the robot is operated through human-guided kinesthetic teaching, where trajectories are generated by manually dragging the arm and subsequently recorded via interpolated playback. During evaluation, the robot is controlled by our ReViP to autonomously execute the specified manipulation tasks. To provide visual observations, we employ two ORBBEC Femto Bolt RGB-D cameras, positioned to capture both first-person and third-person viewpoints.

Tasks and Datasets. Our dataset includes two manipula-

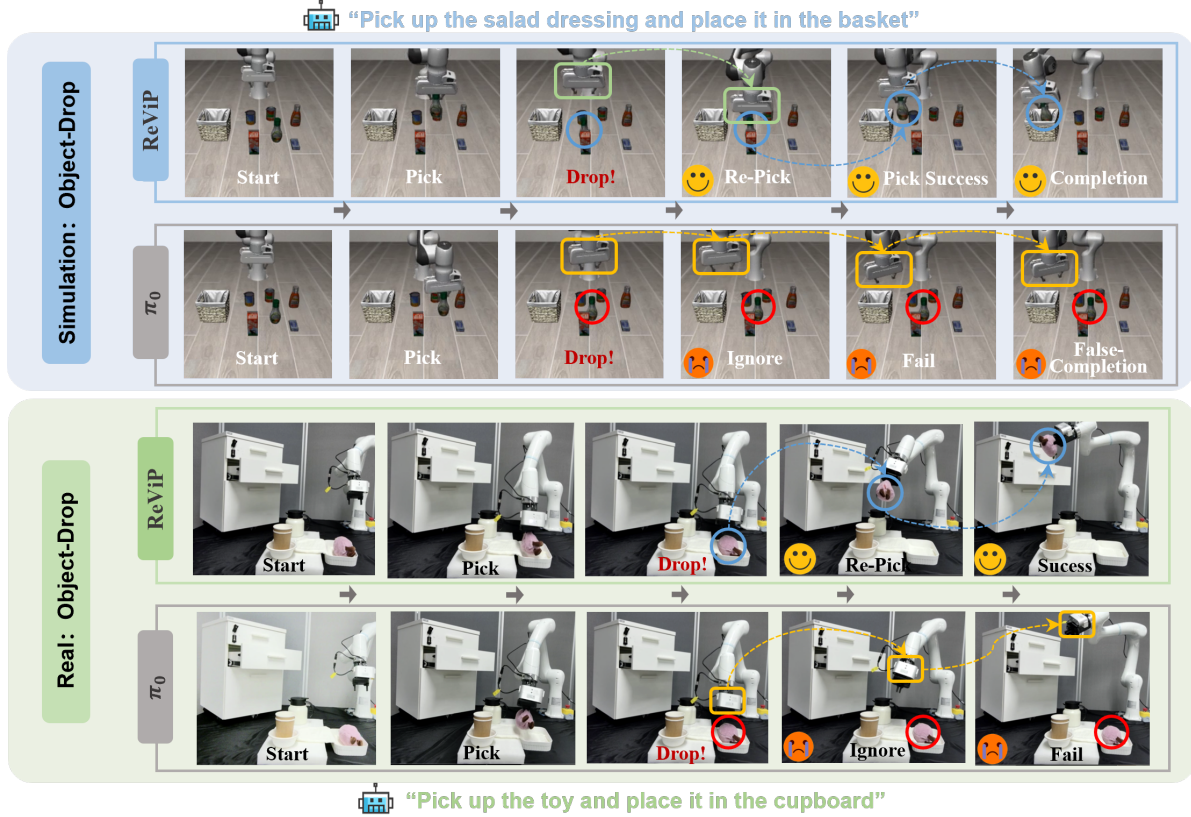


Figure 4. Qualitative comparisons on our False Completion benchmark with Object Drop settings (above: simulation, below: real-world). For simulation, ReViP detects the object drop during execution, and successfully re-picks the target (salad dressing), achieving a true completion \odot , while π_0 fails to react to the clear visual failure and continues executing a state-dominant bias, resulting in false completion \circlearrowleft . In the real world, ReViP can also retrieve the toy when it falls, but π_0 still fails to respond correctly.

Table 4. **Experimental Results of Real-World Experiments.** Success rates (SR) are reported. The best result is shown in **bold**, and ReViP reaches the highest average SR across all real-world settings.

Methods	Object Placement		Drawer Manipulation			Average SR \uparrow
	Cup \rightarrow Box	+Drop	Toy \rightarrow Drawer	+Close	+Drop	
π_0 [5]	4/10	1/10	2/10	8/10	2/10	34%
π_0 -Fast [27]	2/10	1/10	0/10	5/10	1/10	18%
ReViP	6/10	4/10	5/10	10/10	5/10	60%

tion tasks with three different perturbations: Drop, Swap, and Relayout, as described below. (1) *Pick & Place*: This task setup is designed to evaluate the robustness of VLA against visual distractions. The environment contains multiple white distractor objects and the VLA must accurately localize and manipulate the target object. (2) *Drawer Manipulation*: This task tests the VLA model’s ability to handle long-horizon sequences, requiring the model to understand the interaction dynamics within the scene and execute a series of actions in the correct order. Further details can be found in the supplemental materials.

Baseline. In real-world experiments, we compare ReViP

with two SOTA methods, π_0 [5] and π_0 -Fast [27], to assess its performance in handling multi-distractor scenarios and its error-correction ability in long-horizon tasks.

Quantitative Results We conduct real-world training and evaluation for π_0 and π_0 -Fast. As shown in Table 4, ReViP achieves the highest sub-task success rate of 60% and overall success rate in both tasks. Under additional disturbances, ReViP is able to detect that the target object has been dropped and autonomously return to re-grasp it.

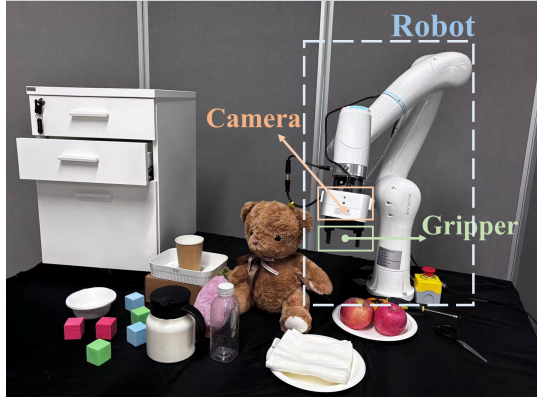


Figure 5. The experimental platform consists of a robot arm, gripper, and cameras. The task objects include multiple targets such as toys and cubes, covering both deformable and rigid items. Data collection and model inference are conducted using RGB-D cameras from both first-person and third-person viewpoints.

5. Conclusion

In this paper, we propose ReViP, a novel VLA framework designed with vision-proprioception rebalance to address the false completion problem. ReViP introduces additional relative task-environment priors, i.e., task-centric visual cues, to adaptively modulate the coupling between semantic perception and proprioceptive dynamics, thereby enhancing visual grounding and robustness under perturbations. Additionally, we propose a benchmark suite for systematically evaluating false completion. Extensive experiments on both simulation and real-world settings demonstrate the effectiveness of ReViP, highlighting the advantages of vision-proprioception rebalancing.

References

- [1] Michael Ahn, Anthony Brohan, Noah Brown, Yevgen Chebotar, Omar Cortes, Byron David, Chelsea Finn, Chuyuan Fu, Keerthana Gopalakrishnan, Karol Hausman, Alex Herzog, Daniel Ho, Jasmine Hsu, Julian Ibarz, Brian Ichter, Alex Irpan, Eric Jang, Rosario Jauregui Ruano, Kyle Jeffrey, Sally Jesmonth, Nikhil J Joshi, Ryan Julian, Dmitry Kalashnikov, Yuheng Kuang, Kuang-Huei Lee, Sergey Levine, Yao Lu, Linda Luu, Carolina Parada, Peter Pastor, Jornell Quiambao, Kanishka Rao, Jarek Rettinghouse, Diego Reyes, Pierre Sermanet, Nicolas Sievers, Clayton Tan, Alexander Toshev, Vincent Vanhoucke, Fei Xia, Ted Xiao, Peng Xu, Sichun Xu, Mengyuan Yan, and Andy Zeng. Do as i can, not as i say: Grounding language in robotic affordances. In *International Conference on Robot Learning*, 2023. 3
- [2] Alexander, Karl Pertsch, Suraj Nair, Ashwin Balakrishna, Sudeep Dasari, Siddharth Karamcheti, Soroush Nasiriany, Mohan Kumar Srirama, Lawrence Yunliang Chen, Kirsty Ellis, et al. DROID: A large-scale in-the-wild robot manipulation dataset. In *Robotics: science and systems*, 2024. 2, 3
- [3] Shuai Bai, Keqin Chen, Xuejing Liu, Jialin Wang, Wenbin Ge, Sibo Song, Kai Dang, Peng Wang, Shijie Wang, Jun Tang, Humen Zhong, Yuanzhi Zhu, Mingkun Yang, Zhao-hai Li, Jianqiang Wan, Pengfei Wang, Wei Ding, Zheren Fu, Yiheng Xu, Jiabo Ye, Xi Zhang, Tianbao Xie, Zesen Cheng, Hang Zhang, Zhibo Yang, Haiyang Xu, and Junyang Lin. Qwen2.5-vl technical report, 2025. 4, 1
- [4] Suneel Belkhale, Tianli Ding, Ted Xiao, Pierre Sermanet, Quan Vuong, Jonathan Tompson, Yevgen Chebotar, Debiddatta Dwibedi, and Dorsa Sadigh. Rt-h: Action hierarchies using language. In *Robotics: Science and Systems*, 2024. 3
- [5] Kevin Black, Noah Brown, Danny Driess, Adnan Esmail, Michael Equi, Chelsea Finn, Niccolò Fusai, Lachy Groom, Karol Hausman, Brian Ichter, Szymon Jakubczak, Tim Jones, Liyiming Ke, Sergey Levine, Adrian Li-Bell, Mohith Mothukuri, Suraj Nair, Karl Pertsch, Lucy Xiaoyang Shi, James Tanner, Quan Vuong, Anna Walling, Haohuan Wang, and Ury Zhilinsky. pi_0: A vision-language-action flow model for general robot control. *Robotics: Science and Systems*, 2025. 2, 3, 5, 6, 7, 8, 1
- [6] Anthony Brohan, Noah Brown, Justice Carbajal, Yevgen Chebotar, Joseph Dabis, Chelsea Finn, Keerthana Gopalakrishnan, Karol Hausman, Alexander Herzog, Jasmine Hsu, Julian Ibarz, Brian Ichter, Alex Irpan, Tomas Jackson, Sally Jesmonth, Nikhil J. Joshi, Ryan Julian, Dmitry Kalashnikov, Yuheng Kuang, Isabel Leal, Kuang-Huei Lee, Sergey Levine, Yao Lu, Utsav Malla, Deeksha Manjunath, Igor Mordatch, Ofir Nachum, Carolina Parada, Jodilyn Peralta, Emily Perez, Karl Pertsch, Jornell Quiambao, Kanishka Rao, Michael S. Ryoo, Grecia Salazar, Pannag R. Sanketi, Kevin Sayed, Jaspia Singh, Sumedh Sontakke, Austin Stone, Clayton Tan, Huong T. Tran, Vincent Vanhoucke, Steve Vega, Quan Vuong, Fei Xia, Ted Xiao, Peng Xu, Sichun Xu, Tianhe Yu, and Brianna Zitkovich. Rt-1: Robotics transformer for real-world control at scale. *Robotics: Science and Systems*, 2023. 3
- [7] Qingwen Bu, Yanting Yang, Jisong Cai, Shenyuan Gao, Guanghui Ren, Maoqing Yao, Ping Luo, and Hongyang Li. Univla: Learning to act anywhere with task-centric latent actions. In *Robotics: Science and Systems*, 2025. 5, 6, 7
- [8] Tianxing Chen, Zanxin Chen, Baijun Chen, Zijian Cai, Yibin Liu, Zixuan Li, Qiwei Liang, Xianliang Lin, Yiheng Ge, Zhenyu Gu, et al. Robotwin 2.0: A scalable data generator and benchmark with strong domain randomization for robust bimanual robotic manipulation, 2025. 2, 6, 7, 4
- [9] Yuqing Du, Ksenia Konyushkova, Misha Denil, Akhil Raju, Jessica Landon, Felix Hill, Nando de Freitas, and Serkan Cabi. Vision-language models as success detectors. In *Conference on Lifelong Learning Agents*, 2023. 3
- [10] Jiafei Duan, Wilbert Pumacay, Nishanth Kumar, Yi Ru Wang, Shulin Tian, Wentao Yuan, Ranjay Krishna, Dieter Fox, Ajay Mandlekar, and Yijie Guo. Aha: A vision-language-model for detecting and reasoning over failures in robotic manipulation. In *International Conference on Learning Representations*, 2025. 3
- [11] Asher J. Hancock, Xindi Wu, Lihan Zha, Olga Russakovsky, and Anirudha Majumdar. Actions as language: Fine-tuning vlms into vlas without catastrophic forgetting, 2025. 3

[12] Zhi Hou, Tianyi Zhang, Yuwen Xiong, Haonan Duan, Hengjun Pu, Ronglei Tong, Chengyang Zhao, Xizhou Zhu, Yu Qiao, Jifeng Dai, and Yuntao Chen. Dita: Scaling diffusion transformer for generalist vision-language-action pol icy. In *International Conference on Computer Vision*, 2025. 2, 3

[13] Wenlong Huang, Fei Xia, Ted Xiao, Harris Chan, Jacky Liang, Pete Florence, Andy Zeng, Jonathan Tompson, Igor Mordatch, Yevgen Chebotar, Pierre Sermanet, Noah Brown, Tomas Jackson, Linda Luu, Sergey Levine, Karol Hausman, and Brian Ichter. Inner monologue: Embodied reasoning through planning with language models. In *International Conference on Robot Learning*, 2023. 3

[14] Physical Intelligence, Kevin Black, Noah Brown, James Darpinian, Karan Dhabalia, Danny Driess, Adnan Esmail, Michael Equi, Chelsea Finn, Niccolò Fusai, et al. $\pi_{0.5}$: a vision-language-action model with open-world generalization. In *Conference on Robot Learning*, 2025. 2, 3, 6, 5

[15] Stephen James, Zicong Ma, David Rovick Arrojo, and Andrew J. Davison. Rlbench: The robot learning benchmark & learning environment. *IEEE Robotics and Automation Letters*, 2020. 3

[16] Ziyan Jiang, Rui Meng, Xinyi Yang, Semih Yavuz, Yingbo Zhou, and Wenhua Chen. Vlm2vec: Training vision-language models for massive multimodal embedding tasks. In *International Conference on Learning Representations*, 2024. 4

[17] Moo Jin Kim, Karl Pertsch, Siddharth Karamchetti, Ted Xiao, Ashwin Balakrishna, Suraj Nair, Rafael Rafailov, Ethan Paul Foster, Pannag R. Sanketi, Quan Vuong, Thomas Kollar, Benjamin Burchfiel, Russ Tedrake, Dorsa Sadigh, Sergey Levine, Percy Liang, and Chelsea Finn. Openvla: An open-source vision-language-action model. In *Conference on Robot Learning*, 2024. 2, 5, 7, 4

[18] Moo Jin Kim, Chelsea Finn, and Percy Liang. Fine-tuning vision-language-action models: Optimizing speed and success, 2025. 2, 5, 7

[19] Hao Li, Qi Lv, Rui Shao, Xiang Deng, Yinchuan Li, Jianye HAO, and Liqiang Nie. Star: Learning diverse robot skill abstractions through rotation-augmented vector quantization. In *Forty-second International Conference on Machine Learning*, 2025. 3, 6

[20] Wei Li, Renshan Zhang, Rui Shao, Jie He, and Liqiang Nie. Cogyla: Cognition-aligned vision-language-action model via instruction-driven routing & sparsification. In *Advances in neural information processing systems*, 2025. 3

[21] Yaron Lipman, Ricky T. Q. Chen, Heli Ben-Hamu, Maximilian Nickel, and Matt Le. Flow matching for generative modeling. In *International Conference on Learning Representations*, 2023. 3

[22] Bo Liu, Yifeng Zhu, Chongkai Gao, Yihao Feng, Qiang Liu, Yuke Zhu, and Peter Stone. Libero: Benchmarking knowledge transfer for lifelong robot learning. In *Advances in Neural Information Processing Systems*, 2023. 2, 6, 3

[23] Songming Liu, Lingxuan Wu, Bangguo Li, Hengkai Tan, Huayu Chen, Zhengyi Wang, Ke Xu, Hang Su, and Jun Zhu. RDT-1b: a diffusion foundation model for bimanual manipulation. In *The Thirteenth International Conference on Learning Representations*, 2025. 7

[24] Zhenyang Liu, Yongchong Gu, Sixiao Zheng, Yanwei Fu, Xiangyang Xue, and Yu-Gang Jiang. Trivila: A triple-system-based unified vision-language-action model with episodic world modeling for general robot control, 2025. 3, 6, 7

[25] Rui Meng, Ziyan Jiang, Ye Liu, Mingyi Su, Xinyi Yang, Yuepeng Fu, Can Qin, Zeyuan Chen, Ran Xu, Caiming Xiong, Yingbo Zhou, Wenhua Chen, and Semih Yavuz. Vlm2vec-v2: Advancing multimodal embedding for videos, images, and visual documents, 2025. 4

[26] Abby O'Neill, Abdul Rehman, Abhiram Maddukuri, Abhishek Gupta, Abhishek Padalkar, Abraham Lee, Acorn Pooley, Agrim Gupta, Ajay Mandlekar, Ajinkya Jain, et al. Open x-embodiment: Robotic learning datasets and rt-x models: Open x-embodiment collaboration0. In *International Conference on Robotics and Automation*, 2024. 3

[27] Karl Pertsch, Kyle Stachowicz, Brian Ichter, Danny Driess, Suraj Nair, Quan Vuong, Oier Mees, Chelsea Finn, and Sergey Levine. Fast: Efficient action tokenization for vision-language-action models. In *Robotics: Science and Systems*, 2025. 2, 3, 5, 6, 7, 8

[28] Delin Qu, Haoming Song, Qizhi Chen, Yuanqi Yao, Xinyi Ye, Yan Ding, Zhigang Wang, JiaYuan Gu, Bin Zhao, Dong Wang, et al. Spatialvla: Exploring spatial representations for visual-language-action model. In *Robotics: Science and Systems*, 2025. 2, 3, 6, 7

[29] Eric Tang, Bangding Yang, and Xingyou Song. Understanding LLM embeddings for regression. *Transactions on Machine Learning Research*, 2025. 4

[30] Chongyang Tao, Tao Shen, Shen Gao, Junshuo Zhang, Zhen Li, Kai Hua, Wenpeng Hu, Zhengwei Tao, and Shuai Ma. Llms are also effective embedding models: An in-depth overview, 2025. 4

[31] Yanjie Ze, Gu Zhang, Kangning Zhang, Chenyuan Hu, Muhan Wang, and Huazhe Xu. 3d diffusion policy. *arXiv preprint arXiv:2403.03954*, 2024. 7

[32] Qingqing Zhao, Yao Lu, Moo Jin Kim, Zipeng Fu, Zhuoyang Zhang, Yecheng Wu, Zhaoshuo Li, Qianli Ma, Song Han, Chelsea Finn, Ankur Handa, Tsung-Yi Lin, Gordon Wetzstein, Ming-Yu Liu, and Donglai Xiang. Cot-vla: Visual chain-of-thought reasoning for vision-language-action models. In *Conference on Computer Vision and Pattern Recognition*, 2025. 2, 3, 6, 7

[33] Zhongyi Zhou, Yichen Zhu, Junjie Wen, Chaomin Shen, and Yi Xu. Chatvla-2: Vision-language-action model with open-world embodied reasoning from pretrained knowledge. In *Advances in Neural Information Processing Systems*, 2025. 3

[34] Brianna Zitkovich, Tianhe Yu, Sichun Xu, Peng Xu, Ted Xiao, Fei Xia, Jialin Wu, Paul Wohlhart, Stefan Welker, Ayzaan Wahid, Quan Vuong, Vincent Vanhoucke, Huong T. Tran, Radu Soricu, Anikait Singh, Jaspiar Singh, Pierre Sermanet, Pannag R. Sanketi, Grecia Salazar, Michael S. Ryoo, Krista Reymann, Kanishka Rao, Karl Pertsch, Igor Mordatch, Henryk Michalewski, Yao Lu, Sergey Levine, Lisa Lee, Tsang-Wei Edward Lee, Isabel Leal, Yuheng Kuang, Dmitry Kalashnikov, Ryan Julian, Nikhil J. Joshi,

Alex Irpan, Brian Ichter, Jasmine Hsu, Alexander Herzog, Karol Hausman, Keerthana Gopalakrishnan, Chuyuan Fu, Pete Florence, Chelsea Finn, Kumar Avinava Dubey, Danny Driess, Tianli Ding, Krzysztof Marcin Choromanski, Xi Chen, Yevgen Chebotar, Justice Carbalal, Noah Brown, Anthony Brohan, Montserrat Gonzalez Arenas, and Kehang Han. RT-2: vision-language-action models transfer web knowledge to robotic control. In *Conference on Robot Learning*, 2023. [2](#), [3](#)

ReViP: Reducing False Completion in Vision-Language-Action Models with Vision–Proprioception Rebalance

Supplementary Material

This appendix provides comprehensive supplementary material to support the methodology, analysis, and findings presented in the main paper. It includes implementation details covering model architectures and training configurations, along with additional experimental results and analyses.

6. Additional Implementation Details

6.1. Model Details

Task-Stage Observer. The Task Stage Observer (TSO) is built upon the Qwen 2.5 VL model [3] and is designed to extract structured, observation-grounded task cues that complement the robotic policy. The TSO takes three inputs: the task instruction, the task goal prompt, and a third person observation image that covers the full workspace. This global viewpoint enables reliable retrieval of object level evidence even under perturbations.

To ensure that the TSO produces concise and structured semantics rather than free form scene descriptions, we design a dedicated instruction protocol for the model, as shown in Table 5. This protocol guides the model to enumerate visual evidence, specify stage-wise completion conditions, and infer an explicit task stage description that is aligned with the ongoing trajectory. Following the hidden state aggregation process detailed in Section 3.2 of the main paper, the TSO output is transformed into a single embedding vector of dimension 8192. This vector serves as the task stage representation z_t and is subsequently fed into the Task Stage Enhancer to enable task stage feature-wise modulation in ReViP.

Task-Stage Enhancer. In ReViP, the Task Stage Observer outputs a task stage representation $z_t \in \mathbb{R}^{8192}$, which is processed by a lightweight bottleneck network to produce the modulation parameters (γ_t, β_t) . The mapping $h(\cdot)$ is implemented as a two-layer MLP with SiLU activations. To maintain stable training, the final projection uses a Xavier uniform initializer scaled by 0.01 with zero initialized biases, so that TS-FiLM behaves close to identity at the early stage while the learnable scalar α gradually adjusts the modulation strength. The resulting $\gamma_t, \beta_t \in \mathbb{R}^D$ are broadcast across tokens and applied to the concatenated vision and language prefix P_t following Eq. (5) in main paper. Importantly, the binary prefix mask $M_t \in \{0, 1\}^{B \times S}$ is applied after modulation to ensure that TS-FiLM only affects valid prefix tokens and fully preserves the padding structure used by the attention backend.

Attention Mechanism. After applying TS-FiLM to obtain the modulated prefix \tilde{P}_t , the tokens are fed into the vision language backbone together with a suffix sequence that contains the state token and the diffusion conditioned noisy action tokens. Let $S_t \in \mathbb{R}^{B \times 1 \times D}$ denote the state token and $A_t \in \mathbb{R}^{B \times H \times D}$ denote the sequence of action and timestep tokens. Then, the action generator’s input X_t can be defined as follows:

$$X_t = [\tilde{P}_t; S_t; A_t] \in \mathbb{R}^{B \times L \times D}, \quad (10)$$

where $L = S + 1 + H$ is the total token length.

Self attention is then applied over X_t with a block structured attention mask \mathcal{M}_t^A that encodes the prefix style interaction pattern inherited from the VLA backbone:

$$H_t = \text{Attn}(Q(X_t), K(X_t), V(X_t); \mathcal{M}_t^A). \quad (11)$$

Prefix tokens in \tilde{P}_t attend to each other across vision and language, but do not attend to the suffix tokens. In contrast, the suffix tokens in S_t and A_t are allowed to attend to all prefix tokens as well as to the appropriate subset of previous suffix tokens according to the autoregressive part of \mathcal{M}_t^A . The binary prefix mask M_t is applied after TS-FiLM so that only valid prefix positions contribute to Q , K , and V , and padding tokens remain completely excluded. This design lets the diffusion head integrate task stage modulated visual context with proprioceptive state and time dependent action information, while keeping the original routing and padding structure of the attention mechanism unchanged during both training and inference.

6.2. Training Details.

Training Setup. We adopt π_0 [5] as the backbone model with full parameter fine-tuning and set the action chunk size to $K = 50$. The model is trained for 60k steps with a batch size of 32. The learning rate follows a cosine decay schedule with 3,000 warmup steps, increasing to a peak of 2.0×10^{-5} and then decaying to a final learning rate of 2.0×10^{-6} . We use the AdamW optimizer with gradient clipping set to 1.0 and apply an exponential moving average (EMA) with a decay value of 0.999.

To avoid excessive training latency caused by online task-stage extraction, we preprocess the entire dataset using the Task-Stage Observer before training. For every action step, we extract the corresponding task-stage intention and store it as part of the training annotations. During training, the task-stage cues are injected into ReViP to provide explicit task-stage guidance, enabling the model to more effectively rebalance visual and proprioceptive features. At

Table 5. Instruction details for the Task Stage Observer.

Component	Content
System Prompt	You are an expert robot task assistant, integrated with a robot arm capable of executing physical actions in the real world. Based on the task goal and observation, provide the additional task-stage information to the robot in a structured and precise way.
Instruction Rules	<ul style="list-style-type: none"> • LIST the current state of all relevant objects (robot arm, scene objects) as visual evidence. • DEFINE clear completion conditions for each task stage. • Determine the current <code>task_stage_cues</code> based on object states and describe it as an ongoing action.
Input Fields	<p>Task Goal: <code>{task_goal}</code></p> <p>Observation: <code>{Third person view image}</code></p>
Output Format	<pre>{ "visual_evidence": ["<evidence_1>", "..."], "task_stage_cues": "<task_stage_cues>"}</pre>

inference time, task-stage intention is computed online by the Task-Stage Observer and fed into ReViP in real time.

7. Additional Experiments Details

7.1. False Completion Benchmark Suite Details

False completion arises when external disturbances or unintended robot actions invalidate the ongoing plan while the robot still declares success. To study state-dominant bias and visually apparent false completions in a controlled manner, we construct a False Completion Benchmark Suite on top of LIBERO that injects targeted perturbations and probes complementary aspects of the phenomenon.

We consider three perturbation sources that commonly induce false completion: *Object Drop*, *Distractor Swap*, and *Object Relayout*. Together they form a suite of **8 manipulation tasks** that constitute the proposed False Completion Benchmark. The instruction remains fixed, and only the environment state is perturbed either at the start of the episode or during execution. This disturbance design prevents success via replaying demonstrations like proprioceptive trajectories and instead compels policies to rely on current visual evidence for progress checking and replanning. An overview of all tasks, including representative visualizations and the corresponding language instructions, is provided in Table 6. Below, we detail the three perturbation families.

Object Drop. This setting tests recovery from unexpected displacement and exposes false completion most directly. We instantiate three variants that differ in object scale and contact context, which in total yield five tasks:

- *Small Object Drop*: a piece of cheese and a block of butter are grasped and then forcibly dropped onto the table, requiring the policy to visually re-detect the fallen small

object and regrasp it.

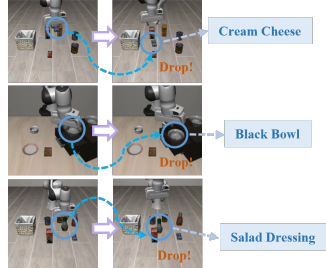
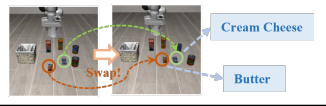
- *Large Object Drop*: a bottle of salad dressing and a carton of orange juice are lifted and then dropped, which introduces longer trajectories and larger motion amplitude compared with small object cases.
- *Bowl Drop in Cabinet*: a bowl is dropped inside a cabinet with occlusion and contact constraints, and the policy needs to visually localize the fallen bowl and complete the task under clutter and limited visibility.

Distractor Swap. This setting evaluates whether the policy detects that two visually similar objects have exchanged positions rather than replaying a proprioception-driven trajectory. The initial poses of the target and a visually similar distractor are swapped while the instruction remains fixed. Concretely, cheese and butter exchange locations after an initial movement phase, and the policy must complete the original instruction with respect to the correct target object. This produces two tasks that differ only in which object is specified as the linguistic target.

Object Relayout. This setting breaks demonstration-specific spatial priors while preserving the linguistic target. The target object and its goal region are jointly relocated to new feasible positions within the workspace. The policy is therefore required to update its plan based on the current visual configuration rather than relying on stale internal state or memorized spatial layouts. In our benchmark, this gives one relayout task that relocates both the target and its goal surface.

Overall, the three perturbation families jointly emphasize visual grounding, continuous progress monitoring, and effective replanning under distribution shifts that frequently result in false completions. The suite provides a focused and diagnostic evaluation framework for VLA models, isolating failure modes that arise when policies overly trust in-

Table 6. Overview of the False Completion Benchmark Suite. The suite contains eight LIBERO manipulation tasks constructed from three perturbation families: Object Drop, Distractor Swap, and Object Relayout. For each perturbation type, we provide representative visual examples together with the corresponding language instructions. The target object is highlighted in **purple** and the goal region is highlighted in **teal**.

Type	Instruction	Visualization Example
Object Drop	<p>❶ Pick up the butter and place it in the basket ❷ Pick up the cream cheese and place it in the basket ❸ Pick up the salad dressing and place it in the basket ❹ Pick up the orange juice and place it in the basket ❺ Pick up the black bowl in the top drawer of the wooden cabinet and place it on the plate</p>	
Distractor Swap	<p>❻ Pick up the butter and place it in the basket. ❼ Pick up the cream cheese and place it in the basket.</p>	
Object Relayout	<p>❽ Pick up the black bowl next to the plate and place it on the plate.</p>	

ternal state progression in the presence of visually apparent disturbances.

7.2. Task Definitions and Evaluation Settings

For all tasks in the False Completion Benchmark Suite, an episode is considered successful only when the agent completes the instructed goal within the predefined step budget. Any premature termination or incorrect placement is counted as failure, even if the policy internally declares success.

Step Budget. The three perturbation families differ in whether the disturbance introduces additional action requirements. For Distractor Swap and Object Relayout, the perturbation only alters the initial scene configuration without increasing manipulation complexity. The number of required actions remains comparable to the original LIBERO tasks, and therefore, the maximum episode length is kept unchanged. In contrast, Object Drop requires the agent to detect the unexpected displacement, relocate the fallen object, and perform an additional re-pick action. This introduces extra motion beyond the demonstration regime. To ensure that policies have sufficient budget to perform recovery, we extend the maximum step limit by an additional 30 to 50 steps, depending on the specific drop variant.

Drop Trigger Rule. For Object Drop tasks, we design a deterministic and reproducible drop triggering mechanism to guarantee fair comparisons across models. A drop event is initiated only when the agent maintains a continuous gripper closing state for a fixed duration, indicating that the ob-

ject has been securely grasped and lifted. Once this condition is satisfied, the environment forces the gripper to open, causing the object to fall from a consistent spatial location. This rule ensures that all models experience the same drop timing and position, removes stochasticity, and isolates the evaluation of false completion behavior to perception and decision making rather than random disturbances.

Fairness Across Perturbations. For Distractor Swap and Object Relayout, perturbations are applied deterministically at environment initialization. Since the instruction remains unchanged and the agent starts from the same initial state distribution, all models operate under identical scene configurations. For Object Drop, the deterministic drop trigger further ensures that each model receives an identical disturbance during execution. Together, these settings guarantee that the benchmark provides a controlled and strictly fair evaluation of policies under visually apparent distribution shifts that may induce false completion.

7.3. LIBERO & RoboTwin 2.0 Benchmark Details

LIBERO Simulation Benchmark. We evaluate ReViP in the LIBERO simulation benchmark [22], a standardized collection of language-conditioned robotic manipulation tasks designed to probe multimodal grounding, visual reasoning, and action generation. Compared with earlier platforms such as RLBench [15], LIBERO provides richer language instructions, more diverse scene layouts, and a broader range of object-level interactions, making it a more suitable testbed for evaluating vision language action mod-

els.

LIBERO consists of four curated task suites: Spatial, Object, Goal, and Long. Each suite contains ten manipulation tasks accompanied by 50 human teleoperated demonstrations. These suites are designed to decouple different aspects of visuomotor reasoning:

- **LIBERO Spatial** tests spatial reasoning by placing identical objects in varying spatial configurations. Success requires interpreting relations such as left, right, in front of, or behind as described in the instruction.
- **LIBERO Object** evaluates generalization across object categories. While spatial layouts are fixed, the target and distractor objects vary in type, shape, and color, requiring accurate object-level grounding from both vision and language.
- **LIBERO Goal** probes goal-oriented understanding by varying the goal specification while holding object identities and spatial layouts constant. Fine-grained semantic distinctions in instructions must be mapped to distinct manipulation outcomes.
- **LIBERO Long** introduces long-horizon tasks involving multiple intermediate steps, diverse objects, and broader spatial compositions. Successful execution requires perception grounding, semantic tracking, and sequential planning.

ReViP is trained and evaluated under the same standard LIBERO protocol as OpenVLA [17] and π_0 to ensure comparability. By covering spatial reasoning, object identification, goal disambiguation, and long-horizon sequencing, the LIBERO benchmark offers a comprehensive and controlled environment for assessing the robustness and visual grounding capabilities of vision-language action models. This makes LIBERO an appropriate platform for evaluating the contributions of task stage modulation in ReViP.

RoboTwin 2.0 Benchmark. RoboTwin 2.0 [8] is a scalable simulation framework and benchmark for robust bimanual robotic manipulation. It instantiates 50 dual-arm tasks across five robot embodiments and provides a large-scale dataset of clean expert trajectories. At the core of RoboTwin 2.0 is a diverse object library and an automatic expert data synthesis pipeline that uses multimodal language models and simulation in the loop refinement to generate realistic task-level execution code. To enhance sim-to-real transfer and robustness, RoboTwin 2.0 applies structured domain randomization along five axes, including clutter, lighting, background, tabletop height, and language instructions, and defines unified evaluation protocols for dual arm policies[8].

In our study, RoboTwin 2.0 serves as a complementary benchmark to LIBERO and is used to assess whether ReViP extends effectively from single-arm settings to more challenging dual-arm coordination. We select four representative tasks from the 50-task suite that cover typical biman-

ual interaction patterns and object configurations. Following the official RoboTwin 2.0 protocol, we fine-tune each model with 50 clean expert demonstrations per task and evaluate it with 100 rollouts under the Hard setting with domain randomization. This evaluation regime imposes a strong robustness requirement and provides a stringent test of the compared vision language action policies.

7.4. Real-World Setup

Our real-world experiments are performed on a 6-DoF ROKAE robotic arm equipped with a JODELL parallel-jaw gripper. We collect real-world successful demonstration trajectories for the Robot Arm via manually moving the robot along the desired path. For all tasks, we gather 50 expert demonstrations. At each control step, the policy receives a main image and wrist image and a 7-dimensional proprioceptive state in joint space (6 joint positions and 1 gripper scalar). The model outputs action joints in an action chunk of 50.

The main paper reports results on two representative manipulation Tasks 1-2, while this appendix extends the evaluation with additional extended Tasks 3-5 designed to assess hardware robustness, scene generalization, and multi-step reasoning ability (please see Section 8.1).

The instructions and descriptions for Tasks 1-2 are provided below:

- *“Pick up the cup on the white plate, then place it inside the white plastic square box”*

This is a structured pick-and-place scenario where the plate serves as a visually distinctive anchor for the target object. The task evaluates basic visual grounding and manipulation stability. In the main paper, this task further includes Drop perturbations to assess the model’s ability to recover from false-completion cases.

- *“Pick up the toy and place it in the open drawer, then close the drawer”*

A multi-stage drawer manipulation task requiring correct sequencing: grasping, placing, and completing the closing motion. This task tests long-horizon reasoning, stage transitions, and re-localization when object visibility changes near drawer boundaries.

Drop Trigger Mechanism We evaluate the model’s response to false-completion scenarios using a controlled Drop perturbation. To ensure **repeatability, fairness, and naturalistic failure behavior**, we implement Drop using a hardware-in-the-loop condition:

First, during execution, we continuously monitor the gripper width in real time. Once the gripper closes beyond a threshold, indicating that it has successfully grasped the object, the robot proceeds with the placement trajectory. Then, at a predefined early stage of this motion, we command the gripper to open, causing the object to fall naturally along its original motion path.

Table 7. **Extended Real-World Evaluation on False-Completion and Long-Horizon Robustness.** Success rates (SR) across challenging real-world settings show that ReViP handles false-completion cases and long-horizon tasks more reliably than baseline policies. The best result is highlighted in **bold**.

Methods	Cup Placement			Cube Placement		Drawer Manipulation	Average SR ↑
	Cup → Box	+Drop	+Distractor	Cube → Box	+Distractor	Manipulation	
π_0 [5]	5/10	4/10	3/10	4/10	2/10	4/10	34%
π_0 -Fast [27]	3/10	1/10	2/10	2/10	0/10	6/10	23%
ReViP	9/10	8/10	6/10	7/10	6/10	8/10	73%

8. Supplementary Quantitative Analysis

8.1. Extended Real-World Task Results

Beyond the standard configuration described above, the appendix includes additional hardware and scene generalization experiments to further evaluate the robustness of ReViP under real-world variations not covered in the main paper. To this end, we introduce three additional tasks that involve new backgrounds, different camera hardware, new object categories, and extended multi-step action sequences. In particular, we replace the wrist-mounted cameras with the ORBBEC DaBai DCW module and substitute the tabletop background with a high-contrast green cloth. These changes alter imaging characteristics, depth quality, and background complexity, creating a significantly more challenging perception environment.

The instructions and descriptions for the extended Tasks 3-5 are provided below:

- “*Pick up the cup on the table, then place it inside the white plastic square box*”. This task removes the plate anchor used in the main paper and employs a plain tabletop decorated with a high-contrast green cloth. The modified background introduces strong color bias and lower object–background separability, making target localization more difficult.
- “*Pick up the small red cube on the table, then place it inside the white box*”. A fine-grained manipulation task involving a small, low-profile cube whose visual features are harder to extract under depth noise. Surrounding distractors further increase the challenge, requiring precise visual grounding and accurate grasping.
- “*Pick up the purple toy on the table, then place it into the middle drawer of the cabinet, and finally close the drawer*”. This extended long-horizon task involves grasping, precise placement, and drawer closing. The scene contains up to ten objects of diverse shapes and colors, creating substantial visual clutter. This setting rigorously tests the model’s ability to maintain stable grounding and execute multi-step actions under complex external interference.

Table 7 summarizes the success rates across all extended tasks. The results reveal several consistent trends:

Table 8. **Experimental Results on the Plug-and-Play Capability of Vision–Proprioception Rebalance.** Success rates (SR) across two task suites: Object Drop in False Completion benchmarks & LIBERO 10. ReViP and ReViP_{0.5} consistently improve success rates across both suites. * indicates results from the official GitHub implementation.

Methods	Object-Drop	LIBERO-10
π_0 [5]	37.6%	85.2%
$\pi_{0.5}^*$ [14]	54.4%	92.4%
ReViP	65.2% (\uparrow 27.6%)	92.2% (\uparrow 7.0%)
ReViP _{0.5}	68.2% (\uparrow 13.8%)	95.8% (\uparrow 3.4%)

Cup Placement. ReViP substantially outperforms both π_0 and π_0 -Fast across all variants, especially under Drop and Distractor settings. The improvement highlights ReViP’s stronger ability to recover from false-completion risks (e.g., object drop) and to reject visually similar distractors in cluttered scenes.

Cup Placement. The cube task poses significant difficulty due to the small size and weak geometric features of the target object. While both baselines suffer heavily under distractor interference, ReViP maintains considerably higher success rates, demonstrating improved fine-grained localization and stable visual grounding.

Drawer Manipulation. ReViP also achieves the highest performance on the long-horizon drawer task. Baseline policies frequently exhibit state-dominant behavior, prematurely closing the drawer after empty grasps or proceeding despite misalignment. In contrast, ReViP more reliably detects errors, re-localizes the target, and completes the full multi-step sequence.

Across all real-world settings, ReViP maintains substantially higher robustness under perturbations and complex visual clutter. These results confirm that the proposed vision–proprioception rebalance improves both false-completion resilience and long-horizon execution in challenging, unconstrained environments.

8.2. Study of the Model’s Plug-and-Play Capability

To further evaluate the plug-and-play capability of the *Vision–Proprioception Rebalance* beyond the π_0 [5] back-



Figure 6. Additional qualitative results in simulation on the False-Completion Benchmark, LIBERO-10, and LIBERO-Goal. In the False-Completion Benchmark, ReViP detects the object drop during execution and re-grasps the target, achieving true completion instead of prematurely terminating. On LIBERO-10 and LIBERO-Goal, ReViP consistently completes long-horizon tasks under diverse disturbances, environments, and object configurations. These visualizations highlight the complexity of the tasks and further demonstrate ReViP’s robustness, generalization, and execution capabilities.

bone used in ReViP, we extend our framework to another state-of-the-art VLA architecture, $\pi_{0.5}$ [14]. We instantiate ReViP on $\pi_{0.5}$, denoted ReViP $_{0.5}$ by integrating the same Task-Stage Observer, Task-Stage Enhancer, and TS-FiLM pipeline, without adding any extra modules or backbone-specific tuning. This setup examines whether the proposed task-stage cues injection functions in a plug-and-play manner across different policy formulations and whether the benefits observed in ReViP naturally transfer to new architectures.

For evaluation, we adopt two challenging task suites that probe complementary aspects of robustness: (i) *Ob-*

ject Drop, containing five representative false-completion tasks requiring failure recovery, and (ii) LIBERO-10, a long-horizon manipulation suite demanding consistent grounding and precise action sequencing. Both suites remain identical across backbones to ensure fair comparison.

As shown in Table 8, ReViP and ReViP $_{0.5}$ consistently improve success rates across both task suites on their respective backbones, π_0 and $\pi_{0.5}$. On the π_0 backbone, ReViP achieves improvements of 27.6% on Object Drop and 7.0% on LIBERO-10. When transferred to $\pi_{0.5}$, the same design further yields gains of 13.8% on Object Drop and 7.0% on LIBERO-10. These results demonstrate that

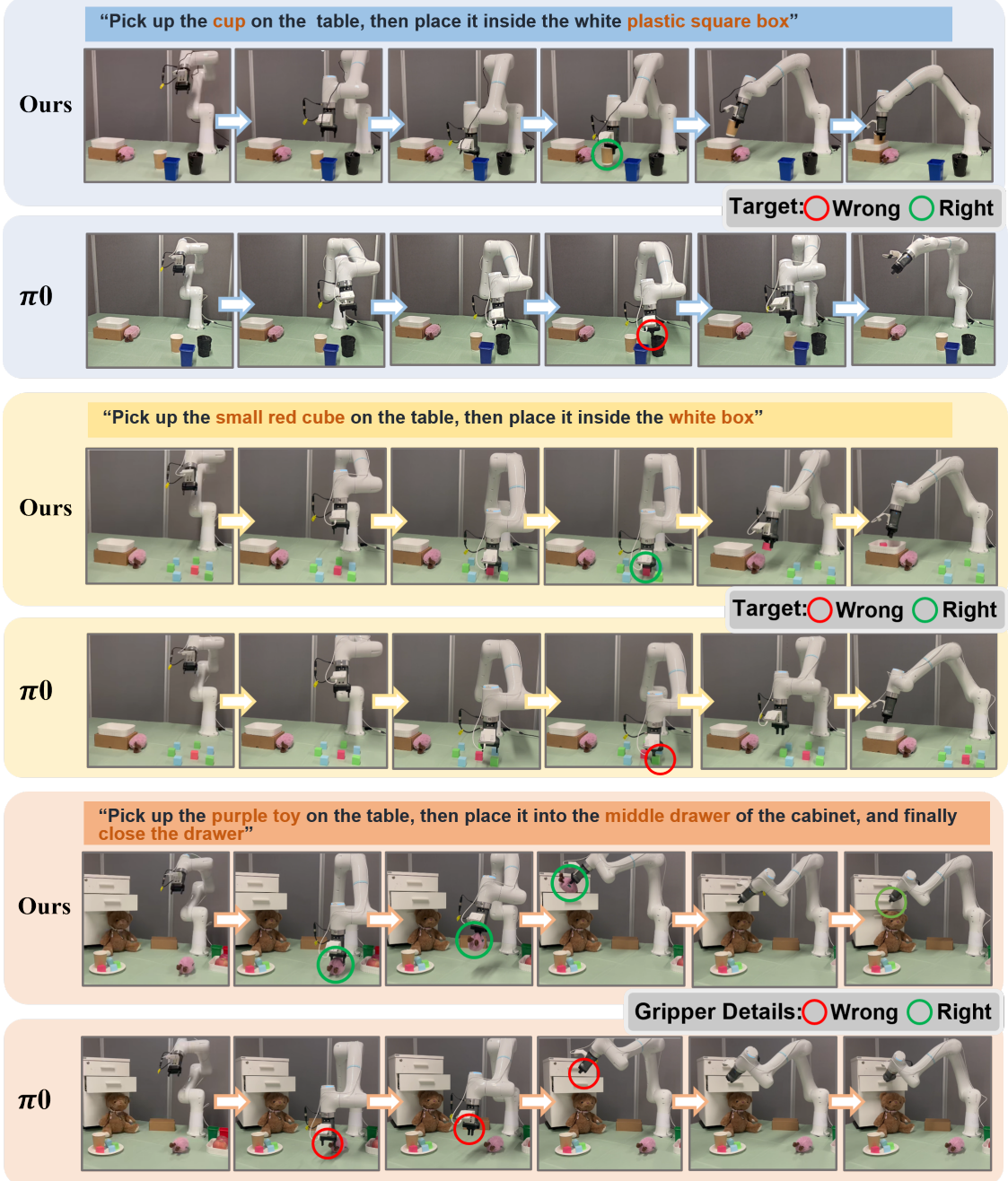


Figure 7. Additional qualitative real-world comparisons between ReViP and π_0 on challenging false-completion scenarios and long-horizon manipulation tasks. ReViP accurately identifies the correct target in cluttered scenes and avoids mis-grasp-induced false completion, while π_0 is easily confused by distractors. For long-horizon drawer tasks, ReViP re-localizes the target and completes the full sequence, whereas π_0 often proceeds with incorrect state-driven actions. The corresponding videos are provided in the supplementary materials.

task-stage conditioning through structured visual evidence functions effectively in a plug-and-play fashion across different VLA architectures, indicating that the proposed vision–proprioception rebalance mechanism is broadly applicable and **not tied to any specific backbone**.

9. Supplementary Qualitative Analysis

We present additional qualitative results from both simulation and real-world experiments, focusing on challenging false-completion scenarios and demonstrating ReViP’s improved robustness, generalization, and execution quality.

9.1. Additional Visualizations of Simulation Results

As shown in Figure 6, we present additional simulation results on both the false-completion benchmark and LIBERO. The model consistently completes multi-step tasks under diverse false-completion disturbances, environments, and object configurations. These visualizations highlight the complexity of the tasks and further demonstrate ReViP’s generalization and execution capabilities.

9.2. Additional Visualizations of Real-World Results

Figure 7 provides qualitative comparisons between ReViP and the baseline π_0 across two representative real-world settings: false-completion scenarios and long-horizon manipulation tasks. The visualizations highlight how ReViP maintains correct visual grounding and robust task progression.

In cluttered environments containing many distractors with highly similar appearance, ReViP accurately identifies the true target object, such as distinguishing the intended cup or red cube from visually similar items. This allows ReViP to execute the correct grasping action. In contrast, π_0 is frequently misled and grasps an incorrect object, which triggers an incorrect stage transition and results in a typical false-completion failure despite clear visual evidence of mis-grasp.

For complex long-horizon manipulation tasks, π_0 often follows internal state progression rather than visual feedback. This leads to errors such as pushing or closing the cabinet even when the gripper is empty, ultimately causing task failure. ReViP detects these inconsistencies, re-localizes the missing target, and then completes the full sequence of grasping, placing, and cabinet operations.

These qualitative examples show that ReViP mitigates false-completion behaviors and significantly improves long-horizon task reliability through better integration of visual observations. The corresponding real-world videos are provided in the supplementary materials.